

Cross Polarized 2x2 LTE MIMO System for Automotive Shark Fin Application

Djordje Preradovic and Daniel N. Aloi

Department of Electrical and Computer Engineering
Oakland University, Rochester, MI 48309, USA
dprerado@oakland.edu, aloi@oakland.edu

Abstract — In this research we propose two orthogonally placed FR4 printed planar monopole antenna elements for use in the automobile roof top shark fin antenna for LTE MIMO applications. The discussed MIMO antenna system is designed to cover the worldwide LTE frequency band from 698MHz to 2700MHz. The goal of this research is to achieve satisfactory MIMO performance across the whole band while staying within physical constraints of the shark fin style antenna. The target reflection coefficient (S11) of each element is -6dB. Because of physical constraints of the automotive shark fin design antenna MIMO decorrelation is achieved by cross polarization and small distance separation. Correlation better than -12dB is targeted and achieved in higher bands, while in lower frequency bands antennas would not benefit from MIMO performance. Numerical simulation of the MIMO antenna system is performed using FEKO in order to verify the design parameters. Simulation findings are confirmed by manufacturing antennas and testing in the lab.

Index Terms — Automotive Antennas, LTE (Long Term Evolution), MIMO (Multiple Input Multiple Output), shark fin, wideband.

I. INTRODUCTION

Antennas play a very important role in wireless communication. They are one of the most important components and without them wireless communication would not be possible. With advancement in communication technologies came need for advancement in antenna technologies.

Today's vehicles have an uncompromised need for an internet connection that enables convenience features, cloud connectivity, autonomous driving as well as more than needed over the air updates. Because of both the consumers' desire for more bandwidth as well as the vehicle's future need for more data, the internet connection quickly becomes a bottleneck of wireless communication. Automakers are doing everything in their power to get data bandwidths up to the latest standards that are used in the telecommunications industry.

Long Term Evolution (LTE) is today's standard of choice in mobile communication with 5G coming in the very near future. Even though LTE is a global standard there are challenges in implementing this standard across the world. Depending on the country and its regulatory bodies, different frequencies are utilized for LTE communication around the world. In order to cover global LTE communication, one needs to design an antenna that would operate with very wide bandwidth. To cover major markets around the world the antenna needs to be operational in following bands 698-960MHz and 1700MHz-2700MHz. In the United States (US) the bandwidth is slightly less from 700-800MHz and from 1800-2355MHz.

Due to the compact size of today's shark fin antennas, antenna designers typically create antennas that rely on different ways to compensate for lack of physical size. These compromises consist of creating complex 3D structures or creating inverted F antennas [1]. Designs are listed in [2], [3], [4]. These antennas although compact in size typically do not have omnidirectional radiation patterns and have limited gain at lower frequencies. Passive gain of the antenna mostly depends on the antenna height above the ground plane. Designs that have good radiation pattern shapes and wide bandwidth are typically large as seen in [5], and do not fit within the mechanical constraints of a shark fin. Other solutions have sufficient performance, but largely ignore LTE band 12 that operates as low as 698MHz in the USA [1]. In addition to the challenge of very wide bandwidth, we also have a challenge of designing a system comprising of multiple antennas in order to increase throughput. Such a system is called multiple input multiple output (MIMO). MIMO is used to multiply capacity of a radio link by using multiple transmitter and receiver paths that are later merged at the radio device. Achieving maximum capacity is only possible if antennas are properly isolated from each other and designed to perform as a pair in a system.

This research focuses on designing a MIMO antenna system that is to be used in an automotive shark fin application.

II. ANTENNA DESIGN

A. Concept and requirements

Our design differs from other designs in the literature as it packages two monopole antennas within the 70mm height constraints of the shark fin antenna. Decorrelation between the antennas is achieved by cross polarization. Two wide band monopole antennas are placed orthogonal to each other and are spaced 25mm apart. Both antennas cover multiple frequency bands from 698MHz to 2700MHz. Our research is novel as it focuses on specific packaging constraints within the automotive shark fin while maintaining highly desired monopole design and achieving the performance needed for a successful LTE communication system.

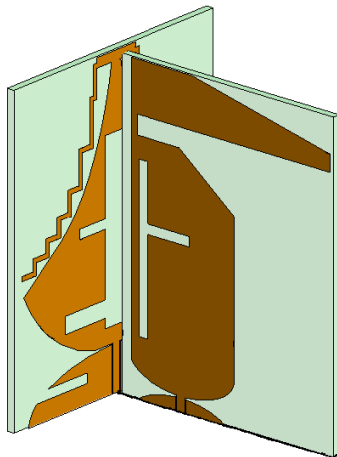


Fig. 1. MIMO antenna system design.

Antenna 1 has a unique tear drop design that follows the cross section of the shark fin and allows it to be placed in the back of the shark fin cover. This area is traditionally not used as often because of cross section constraint. Antennas are typically oriented along the length of the shark fin antenna. Placing multiple antennas for a MIMO system is challenging when trying to minimize the correlation between them as there is not enough space within the cover.

Antennas that operate at low frequencies have a wide top loaded element [5] unlike our antenna that has very narrow tip and is still able to achieve good performance in the 700MHz band. By closely following the cross section of the shark fin we can utilize maximum space within the shark fin by using a monopole structure that typically requires more space compared to other antenna types, an example is the inverted F antenna [1], [6].

For antenna 2 we follow a similar concept to maximize the occupied space in the area that is traditionally empty within the shark fin. This antenna follows the contour of the shark fin cover, reaching its maximum height of 65mm and sloping towards the front.

The top loaded element of the antenna extends forward inside the cover, which allows for large physical size of the antenna to occupy unused space, and while not taking precious circuit board space below for mounting. Space underneath the overhang is typically used for additional antenna elements, such as global positioning system (GPS) or satellite digital audio radio (SDAR). This unique design of the antenna allows for better integration with other services within the shark fin. Figure 1 shows computer aided design (CAD) design of the MIMO system.

B. Modeling and computation

Each antenna is designed individually using simulation with a full-wave, three-dimensional, electromagnetic field solver (FEKO). Before starting with the modeling, we had to decide on the simulation setup. Simulation parameters have large impact on the time it takes to solve the model. Differences in simulation time between coarse and fine mesh model are from a few hours to over a day. The number of frequencies also plays a big impact on simulation duration. In order to quickly evaluate the design, a decision was made to use a coarse mesh model with a smaller number of frequency points at the start of modeling. As we approached closer to desired results, we increased the number of frequency points and fineness of the mesh model. This gave us more accurate results in the end. The typical time to solve the model was few hours with a coarse model and over 24 hours with a finer mesh model. Simulations were performed on an eight-core CPU with 64GB of RAM memory. During the design process we decided to evaluate specific frequencies, sometimes one or a few at the time to evaluate changes that we made without needing to re-simulate the full solution. This allowed for a faster design process during a trial and error method of problem solving.

When modeling a ground plane, it's common practice that a 1m ground plane is used. In our case this presented a large problem, it increased the number of triangles in a mesh and increased the time required to solve the model. What was first initially a modeling problem, became a conscious decision to change design parameter. After evaluating roof structures of current vehicles, we realized that the ground area that is available on the roof is much smaller than 1m in diameter. This was due to the position of the shark fin and large glass openings in the roof. Based off this information we decided to define our ground plane to be 40cm in diameter.

When choosing the materials in the simulation and later in manufacturing we used standard automotive practices as guidelines. This means either choosing a steel structure element or copper printing the antenna on a circuit board. We expected that the antenna design

pattern would get complex with need to closely control dimensions, and as such we have chosen to print the antenna on a circuit board. This would yield more accurate geometric shapes versus cutting the steel.

Now that we have chosen a printed antenna, we selected FR-4 as our dielectric of choice. This is typically a material of choice in the automotive industry as it is low cost and easy to manufacture. Due to cost constraints manufacturers typically do not have strict requirements on the type of prepreg used, which results in various dielectric constants depending on the manufacturer. Before starting on the complex design, we evaluated S parameters of the basic wide band monopole while changing the dielectric constant of the FR-4. We evaluated from having no FR-4 to having FR-4 with standard tolerances, from $\epsilon_r=0$ to $\epsilon_r=5$. Other than a slight shift in resonant frequency, we did not see a major impact in frequencies up to 2.7GHz. Other parameters we also considered are loss tangent of the material at specific frequencies. Upon evaluation of the FR-4 datasheets, we found that loss tangent becomes a problem at frequencies above 2.7GHz, and we decided that a standard tolerance FR-4 is adequate material to use for our application. We decided to use a nominal dielectric constant of 4.4 for simulations and identified that any shift in frequency can be addressed during the design of the structure.

After the initial requirements and design decisions, antennas were simulated to evaluate performance parameters comprising of radiation patterns, reflection coefficient and gain, to make sure they exhibit good individual performance. After achieving acceptable individual performance, the antennas were combined on a single ground plane and retuned for optimal performance in a MIMO system. Retuning consisted of small dimensional changes and impedance tuning, but it did not change the overall shape of the structure. After optimal performance is achieved in simulation, we proceeded to manufacture the antennas.

C. Manufacturing

Each antenna was ordered and to be printed on 1.6mm FR-4 circuit board with a 1oz copper layer. Unless specifically requested, the dielectric constant can vary slightly depending on the prepreg supplier. Due to cost and availability standard FR4 was ordered. The antenna elements are placed on a 40cm diameter steel ground plane. Each antenna was terminated with a SMA connector for ease of performing measurements. Figure 2 shows a manufactured antenna system.

D. Measurement setup

We measured multiple parameters on the antennas and defined measurement setups. S parameters were

measured on the bench in the lab using two port vector network analyzers (Rohde and Schwarz, ZNB-8). The ground plane with antennas was placed on a foam stand, to eliminate any coupling effects from the environment and the data was recorded. For the antenna pattern and gain we performed radiated measurements in an anechoic chamber on 1-meter ground plane with rolled edges.

We further present design details for each antenna and simulation and measurement data of such a system, as well as steps taken to design MIMO system.

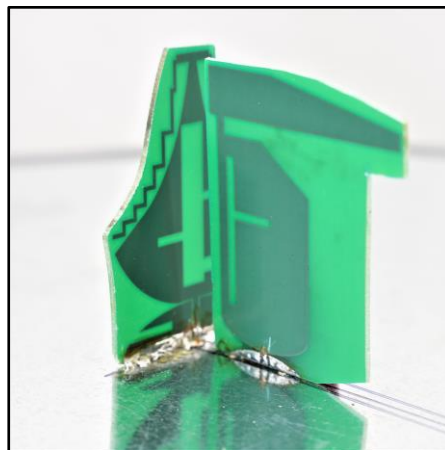


Fig. 2. Manufactured MIMO system.

III. ANTENNA 1

A wideband square monopole antenna, that is known in literature [7], along with our previous designs were used as a starting point in this design. We added a semi-circular base in order to widen the bandwidth of the element. A top loaded meandering element was added to increase electrical size of the antenna in order to make it resonant in the 700MHz frequency band. The idea for a top loaded meandering line came from [8]. Aspects of this design were also taken from our previous work in [9]. When placed next to a secondary antenna the reflection coefficient changed, and it therefore required design optimization in order to optimize overall performance in the system.

We referenced antenna [10] in our design and used it as a guide, further reducing its size. An elliptical base ground is a well-known design element of the ultra-wide band antennas [11]. Target reflection coefficient across the whole band is -6dB or better, except the 2400MHz area that was higher than -6dB. The reflection coefficient improved to better than -6dB when antenna 1 was used in the system together with antenna 2. Major antenna parameters are listed in Table 1 as they relate to the drawing in Fig. 3.

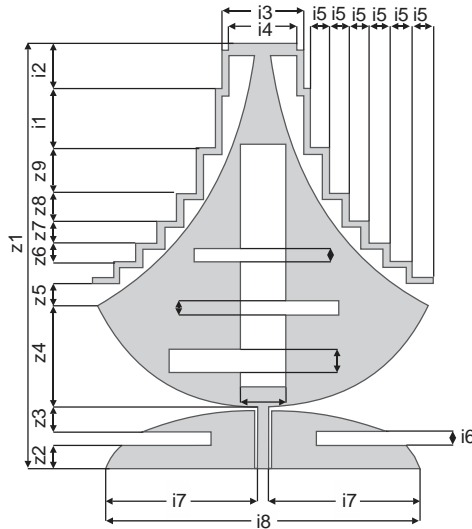


Fig. 3. Antenna 1 dimensions.

Table 1: Antenna 1 parameter

Parameter	Value (mm)	Parameter	Value (mm)
z1	65	i1	9
z2	4	i2	7
z3	3	i3	12.5
z4	16	i4	10
z5	3	i5	3
z6	2.5	i6	2
z7	3.5	i7	24.5
z8	4.25	i8	52
z9	7		

A. Simulation and measurements

Simulation results show that in the lower frequency band from 698-960MHz a reflection coefficient of -6dB is achieved. In the higher band from 1700-2700MHz simulation result show that a reflection coefficient is less than ideal at 2400MHz, this was not reflected in the measurement results where we see reflection coefficient better than -7dB in the higher band. Antenna 1 simulated vs measured reflection coefficient are shown in Fig. 4.

Antenna 1 was manufactured to match the design that was finalized in simulation. A good correlation between the simulated and measured results was obtained in the lower frequency band. On the contrary,

significant differences occurred between the simulated and measured results at the higher band. For antenna 1 we can see that simulation and measurement match from 698MHz to 800MHz with discrepancies between 800MHz and 960MHz. The reflection coefficient trend is shifted in frequency, and while this discrepancy shows some correlation problem between perfect simulation design and manufactured antenna, we can see that overall reflection coefficient on manufactured parts improved in comparison to the simulated data. Some differences are to be expected, and since the overall reflection coefficient improved and meets the previously set requirements, we can proceed with the design on the second antenna and complete MIMO system. In the next iteration of the design this discrepancy will be addressed.

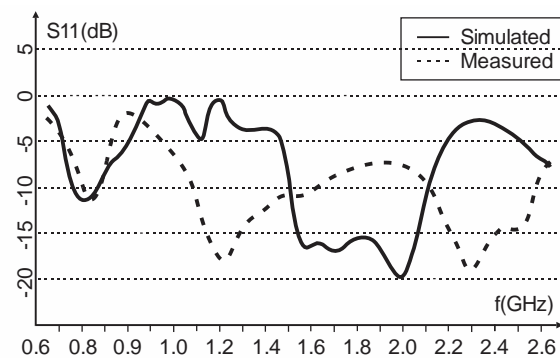


Fig. 4. Antenna 1 - reflection coefficient (S11).

Symmetrical radiation patterns were observed with good coverage around the antenna. Figures 5 (a-d) shows the gain patterns for vertical polarization versus elevation angle at four frequencies across the operating bandwidth while Table 2 shows summary of the maximum vertically polarized gain comparison between simulated and measured results at 30-degree elevations.

Table 2: Total gain – simulated vs measured

Elevation	Freq. (MHz)	Simulated V Max Gain (dB)	Measured V Max Gain (dB)
30 Deg	700	1.04	1.68
30 Deg	1800	3.47	5.95
30 Deg	2300	3.10	3.34
30 Deg	2700	7.14	3.76

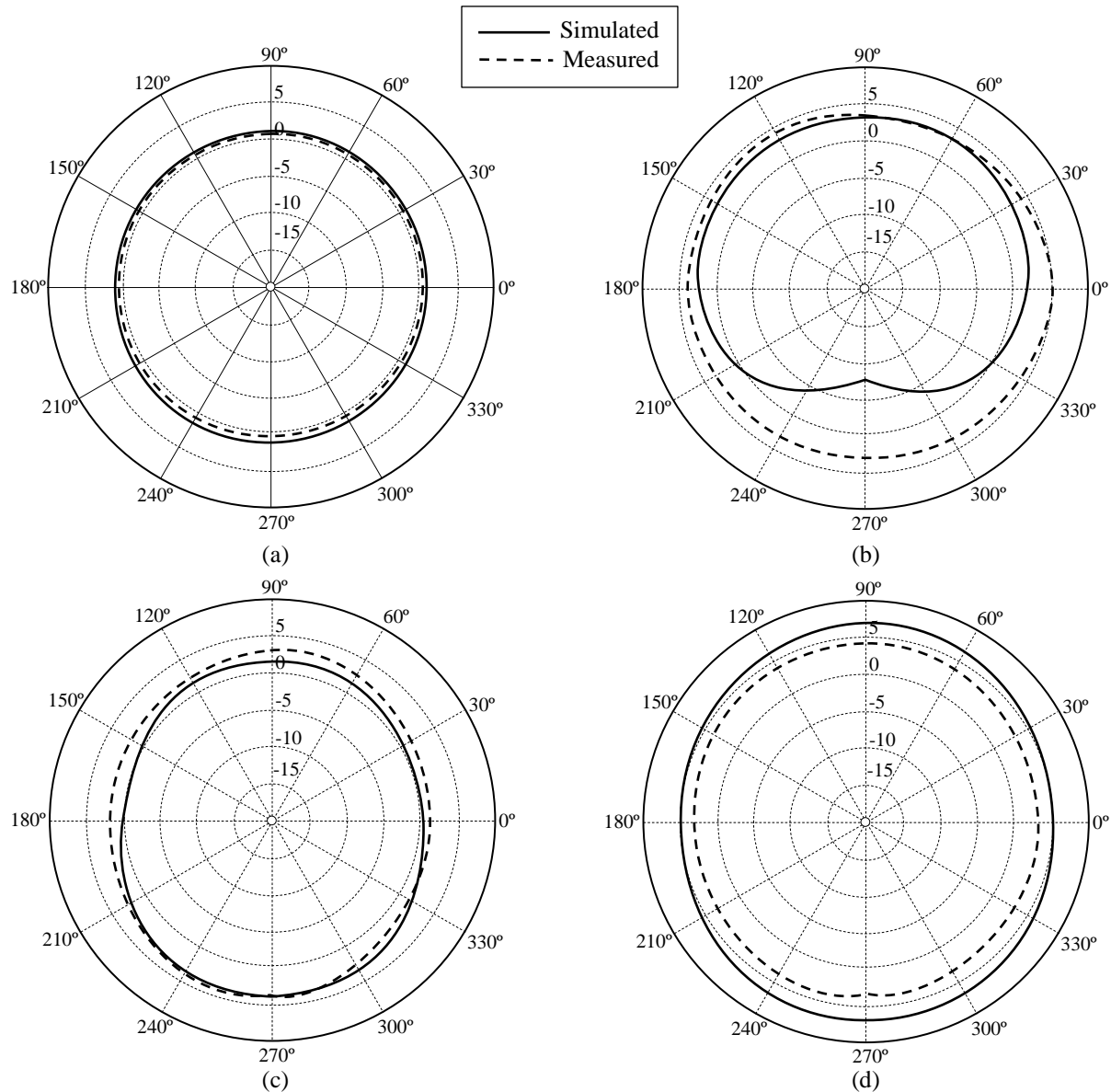


Fig. 5. (a) Antenna 1 – 700MHz radiation pattern, (b) antenna 1 – 1800MHz radiation pattern, (c) antenna 1 – 2300MHz radiation pattern, and (d) antenna 1 – 2700MHz radiation pattern.

IV. ANTENNA 2

Antenna 2 uses a similar structure concept as the first antenna. It is a top loaded monopole structure. The shape of this antenna looks like the Greek capital letter Gamma (Γ). The shape is chosen so that it could fit inside the shark fin antenna and follow the contour of the fin. This design also takes into consideration the distance at which the antenna should be placed in reference to antenna 1 that is placed in the back of the housing. Its back side is flat so that distance between antenna 1 and antenna 2 can be varied for optimal coupling. The top hat of the antenna is designed such that it provides large physical lengths but also allows it to overhang above

other antenna elements such as the GPS and SDAR ceramic patch elements within the shark fin radome. In addition, its narrow base occupies minimal real estate on the circuit board. Figure 6 shows the antenna design and parameters.

This antenna element is placed parallel to the direction of the antenna housing, following the curve of the top of the shark fin while not exceeding the 70mm height requirement. This antenna's feeding structure is 2mm wide and has height of 5mm. A monopole structure is used for its omnidirectional coverage.

Antenna 1 is used as starting reference point, which also based on a wideband square monopole antenna, that

is known in literature [7]. The semicircular base on the bottom is added in order to widen the bandwidth of the element. The top loaded element was added to increase physical size of the antenna in order to make it resonant in the 700MHz frequency band. The idea for top loaded element came from [8]. Through the process of trial and error this antenna has been optimized to perform individually and then in the MIMO system. A target reflection coefficient across the whole band is -6dB or better. Table 3 shows the final dimensions of the antenna 2 as they relate to the Fig. 6.

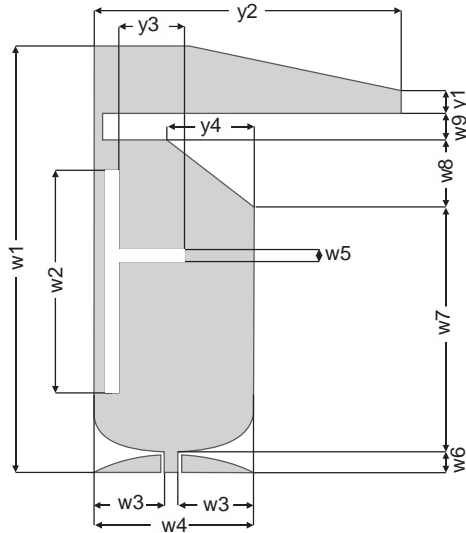


Fig. 6. Antenna 2 dimensions.

Table 3: Antenna 2 parameters

Parameter	Value (mm)	Parameter	Value (mm)
w1	65	w8	10
w2	34	w9	4
w3	10.5	y1	3.5
w4	24	y2	50
w5	2	y3	10
w6	4	y4	13
w7	37		

A. Simulation and measurements

In Fig. 7 we see a comparison between simulated and measured reflection coefficient. The reflection coefficient in the upper (1698-2700MHz) and lower (698-960MHz) frequency bands is better than -6dB. We see that in the lower band, the reflection coefficient closely matches between simulation and measurements. While in the upper band there is a slight discrepancy at 2200MHz, but the requirement of -6dB is still achieved

between simulation and measurements.

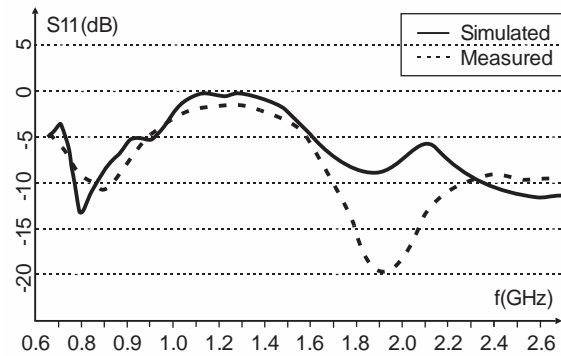


Fig. 7. Antenna 2 – Simulated vs measured reflection coefficient (S11).

Additional measurements were performed on the manufactured parts in order to see how closely they resemble simulation. Radiation pattern and gain measurement have been performed across whole frequency band. In Figs. 8 (a-d) we can see a vertical gain plot at 30-degree elevation. An elevation angle of 30 degrees was chosen as that's typically the maximum angle the vehicle would see to a base station. Table 4 shows a summary of the simulated and measured maximum vertical gain at 30-degree elevation.

Table 4: Total maximum gain simulated vs measured

Azimuth	Freq. (MHz)	Simulated V Max Gain (dB)	Measured V Max Gain (dB)
30 Deg	700	2.34	3.29
30 Deg	1800	3.93	5.70
30 Deg	2300	4.63	6.30
30 Deg	2700	4.15	5.44

V. MIMO

A. MIMO simulation and measurement

The plot in the Fig. 9 shows a comparison between simulated and measured coupling between antenna 1 and antenna 2. Even though we see some difference in the scale of the plot, we can conclude that in the higher band above 1698MHz, plots have similar shape and follow the same trend. Slight differences can be attributed to the measurement setup and differences between the CAD model and real model. In the lower band, we see that plots are similar between 698-765MHz, while there are significant differences from 765-960MHz. We believe that this is also due to differences in physical parts compared to simulation, and difference in grounding that has much greater effect on lower frequency band.

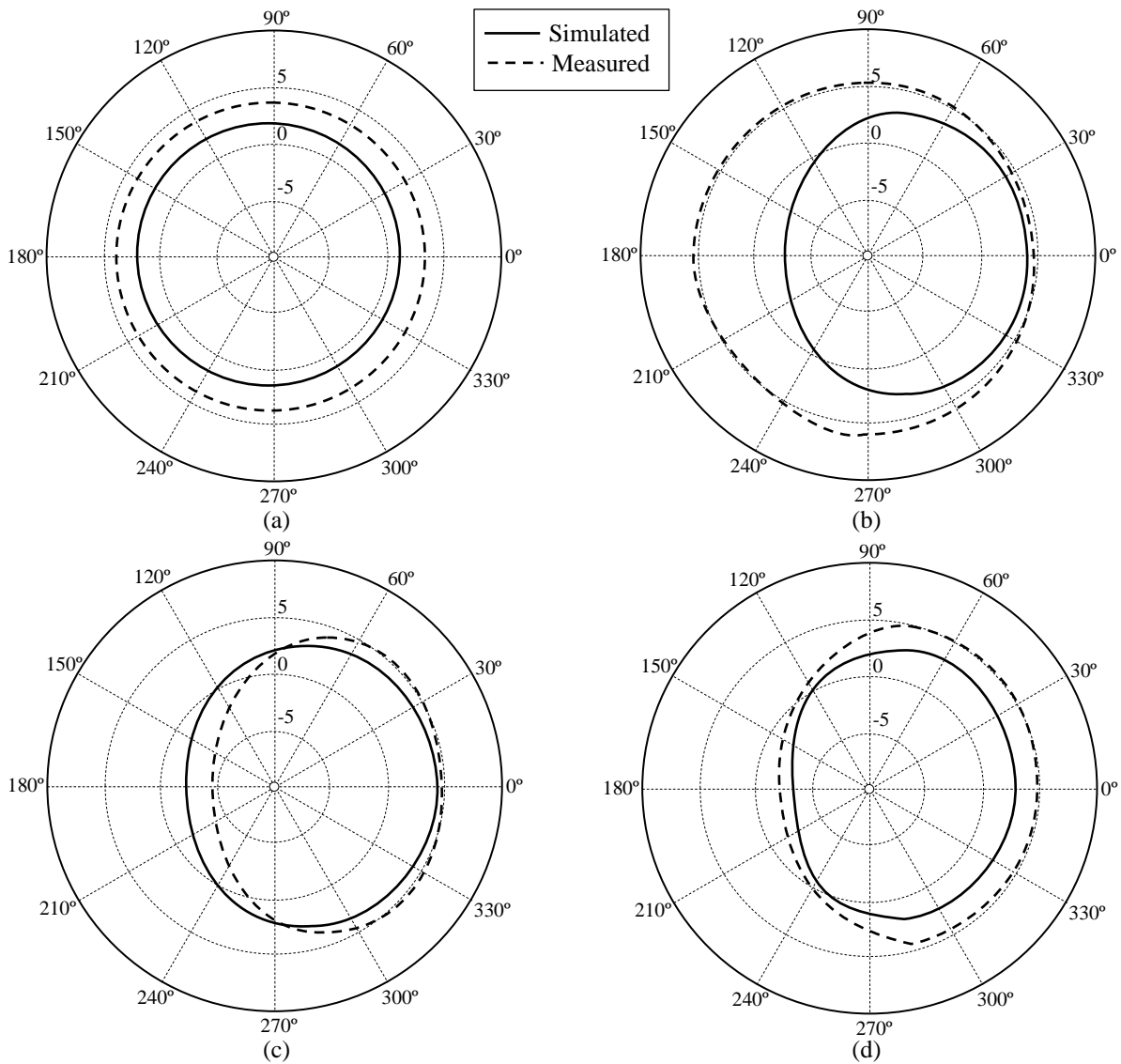


Fig. 8. (a) Antenna 2 – 700MHz radiation pattern, (b) antenna 2 – 1800MHz radiation pattern, (c) antenna 2 – 2300MHz radiation pattern, and (d) antenna 2 – 2700MHz radiation pattern.

Finding a perfect balance of coupling between antennas is a delicate challenge. If antenna performance is good, the coupling is also high which hurts MIMO performance. In this case, both antennas are vertically polarized monopole structures, which means they would have high coupling when separated only by small distance.

This is obvious in lower frequency band where antennas can only achieve -7dB coupling. In this case this would result in unsatisfactory MIMO performance, essentially translating into throughput of a single antenna instead of two antennas.

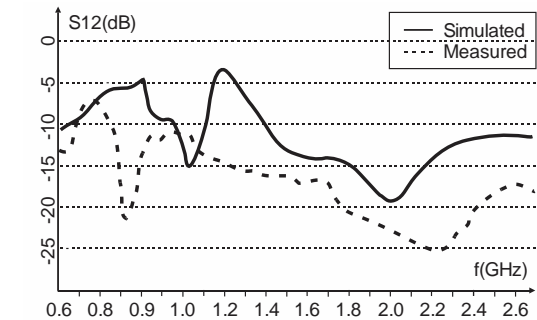


Fig. 9. Simulated and measured antenna coupling (S12).

In Table 5 we show a summary of antenna coupling values at different frequencies throughout the band. Low coupling of less than -12dB is preferred and coupling less than -15dB is achieved in the higher frequency band. This would theoretically double throughput in the higher frequency band above 1698MHz.

Table 5: Simulated vs measured antenna coupling

Freq. (MHz)	Simulated Coupling (dB)	Measured Coupling (dB)
699	-7.75	-7.68
960	-3.65	-11.65
1698	-12.72	-15.83
2500	-10.17	-17.30

We have also evaluated envelope correlation coefficient in both simulation and measurement. Diallo et al. [15] have shown the method to find equivalence between the complex E- filed pattern and the S-parameter of the antenna system under certain circumstances. From the measurements we can see that both antennas have omni directional radiation patterns, which would result in low isolation. In highly efficient antennas we can express envelope correlation coefficient (ECC) in terms of S parameters, as shown in [13] and [15]. Assuming antennas are lossless and tested in uniform multipath environment, equation (1) shows envelope correlation coefficient.

$$\rho_e \cong \frac{|S_{11}S_{12} + S_{22}S_{21}^*|}{(1 - |S_{11}^2 + S_{12}^2|)(1 - |S_{22}^2 + S_{21}^2|)}. \quad (1)$$

From the Fig. 10, we see that simulated and measured results follow the same general trend. In order to have sufficient MIMO performance ECC of 0.5 or less is desired. As also shown earlier, we see that coupling is high in lower frequency band. This is somewhat expected outcome as distance in the antenna in relation to the wavelength is small. In this band antennas would still operate in diversity mode, improving overall performance, but MIMO throughput would not increase. In higher band we see that ECC is less than 0.5, except at 2.5GHz where it is 1. The portion that needs to be further analyzed is using this system for worldwide LTE frequency spectrum. However, such a system can fully utilize MIMO capabilities for a North American market.

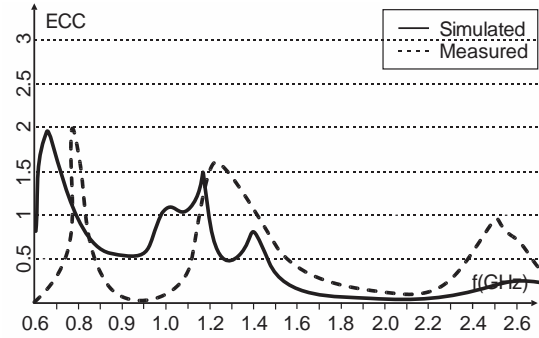


Fig. 10. Simulated and measured ECC of the MIMO system.

VI. CONCLUSION

We see that challenges are in the lower band as expected as the lower frequencies require larger antenna structures. In terms of Antenna 1, differences between simulation and measurement need to be understood and further improvements made to improve performance in the lower frequency band. Antenna 2 performance is satisfactory and does not need to be changed. Performance that we achieved in the system today is sufficient for it to operate in North American LTE bands, and further optimizations are necessary to expand the design to worldwide frequencies.

In terms of the MIMO system performance, isolation is good in the higher frequency band, but it needs to be improved in the lower frequency band. Distance between antennas will be considered when optimizing coupling of the antennas and will be further analyzed. Changes and optimizations to the antenna structure will also be evaluated. Similar tests and antenna position optimization were performed in [12], describing antenna positions within shark fin housing.

There are many ways to design an antenna, this becomes apparent when doing literature survey of different designs. Due to the complexity of antenna structures, test methods, differences in simulation parameters, materials used, and tolerances, it would not be adequate to compare individual parameters of the antenna. Therefore, in Table 6 we give an overview of some of reference designs, with general parameters like antenna type, radiation pattern, size, footprint and implementation feasibility.

Table 6: Reference design comparison

Reference Design	Antenna Type	Bandwidth	Omni Directional Radiation Pattern	Suitable for Shark Fin Style Cover	Minimum Footprint Occupied
Our Design	Monopole	Wide	Yes	Yes	~1224mm ²
[1]	PIFA	Wide	No	Yes	~5000mm ²
[2]	Monopole	Narrow	Yes	No	~2000mm ²
[3]	PIFA	Narrow	No	Yes	~2600mm ²
[5]	Monopole	Wide	Yes	No	~500mm ²
[14]	PIFA	Wide	Yes	Yes	~4030mm ²

REFERENCES

- [1] V. Franchina, A. Michel, P. Nepa, M. Gallo, R. Parolari, A. Polo Filisan, and D. Zamberlan, "A compact 3D antenna for automotive LTE MIMO applications," *2017 IEEE-APS Topical Conference on Antennas and Propagation in Wireless Communications (APWC)*, vol. 7, pp. 326-329, Sep. 2017.
- [2] H. Kim, J. Jeon, M. K. Khattak, S. Kahng, S. Yoo, and E. Shin, "Design of a dual-band LTE MIMO antenna to be embedded in automobiles," *International Symposium on Antenna and Propagation 2015*, Hobart, Tasmania, Australia, vol. 1, pp. 1-3, Nov. 2015.
- [3] O. Y. Kwon, R. Song, and B. S. Kim, "A fully integrated shark-fin antenna for MIMO-LTE, GPS, WLAN, and WAVE applications," *IEEE Antennas Wireless Propagation Letters*, vol. 17, no. 4, pp. 600-603, Apr. 2018.
- [4] A. Michel, P. Nepa, M. Gallo, I. Moro, A. Polo Filisan, and D. Zamberlan, "Printed wideband antenna for LTE band automotive applications," *IEEE Antennas Wireless Propagation Letters*, vol. 16, pp. 1245-1248, Nov. 2016.
- [5] B. Sanz-Izquierdo, S. Jun, and T. B. Baydur, "MIMO LTE vehicular antennas on 3D printed cylindrical forms," *Wideband and Multi-Band Antennas and Arrays for Civil, Security and Military Applications*, pp. 1-5, Dec. 2015.
- [6] T. Mahler, J. Kowalewski, L. Reichardt, and T. Zwick, "Realization of a synthesized compact automotive roof-top LTE antenna," *2013 IEEE International Symposium on Antennas and Propagation & USNC/URSI National Radio Science Meeting*, pp. 2073-2074, July 2013.
- [7] H. R. Hassani and S. M. Mazinani, "Passive microwave components and antennas," pp. 487-510, Apr. 2010.
- [8] Y. Yao, X. Wang, and J. Yu, "Multiband planar monopole antenna for LTE MIMO systems," *International Journal of Antennas and Propagation*, vol. 2012, Article ID 890705, 6 pages, Sep. 2011.
- [9] D. Preradovic and D. N. Aloï, "Ultra wide planar monopole antenna for LTE application in automobile," *2018 IEEE International Conference on Electro/Information Technology (EIT)*, vol. 2018, pp. 774-777, May 2018.
- [10] B. Sanz-izquierdo and R. Leelaratne, "Evaluation of wideband LTE antenna configurations for vehicle applications," *2013 Loughborough Antennas & Propagation Conference (LAPC)*, pp. 383-387, Nov. 2013.
- [11] X. L. Liang, "Ultra wideband antenna and design, ultra wideband - Current status and future trends," pp. 127-147, Oct. 2012.
- [12] T. Lankes, P. Turban, and F. Mierke, "Evaluation and optimization of LTE MIMO antenna configurations in automotive environment," *The 8th European Conference on Antennas and Propagation (EuCAP 2014)*, vol. 7, no. EuCAP, pp. 1100-1104, Apr. 2014.
- [13] B. Auinger, M. Gadringer, A. Tankielun, C. Gagern, and W. Boesch, "On the envelope correlation coefficient of an LTE reference antenna system for band 13," *International Journal of Future Computer and Communication*, vol. 4, no. 1, pp. 13-17, Feb. 2015.
- [14] N. Guan, H. Tayama, M. Ueyama, Y. Yoshijima, and H. Chiba, "A roof automobile module for LTE-MIMO antennas," *2015 IEEE-APS Topical Conference on Antennas and Propagation in Wireless Communications (APWC)*, Turin, pp. 387-391, Sep. 2015.
- [15] A. Diallo, P. Le Thuc, C. Luxey, and R. Starajs, "Diversity characterization of optimized two-antenna systems for UMTS handsets," *EURASIP Journal on Wireless Communications and Networking*, vol. 2, pp. 1-9, Nov. 2007.



Djordje Preradovic, received his Bachelor of Applied Science degree in Electrical Engineering/Communications Option from University of Windsor, Windsor, Ontario, Canada in 2007. Preradovic went on to complete his Master's degree in Electrical and Computer Engineering at Oakland University in 2009, focusing on wireless communications. He started his Ph.D. in Electrical and Computer Engineering in 2010 and became a candidate in 2012.

Since 2008, he worked in the wireless field in the automotive as both hardware and systems engineer. Preradovic worked at Marquardt GmbH, Chrysler Group LLC and is presently working at Continental AG, all in Detroit area. He is currently leading Intelligent Antenna Module and Bluetooth Smart Access product development for the North American Market.



Daniel N. Aloï, received his B.S. (1992), M.S. (1996) and Ph.D. (1999) degrees in Electrical Engineering from Ohio University, located in Athens, Ohio, USA. He served as a Research Assistant from 1995–1999 in the Avionics Engineering Center within the School of Engineering and Computer Science at Ohio University; Summer

Intern at Rockwell International in Cedar Rapids, Iowa, and Senior Project Engineer at OnStar, Incorporated, a subsidiary of General Motors from 2000–2002. He has been employed in the Electrical and Computer Engineering Department at Oakland University in Rochester, Michigan from 2002 until present, currently as Professor and Chair of Electrical and Computer Engineering Department. He is the Founder and Director of the Applied EMAG and Wireless lab at Oakland University. Aloï's research interests reside in area of applied electromagnetics with emphasis on antenna measurements, antenna modeling/analysis and antenna design. He is a member of the Institute of Navigation and is a senior member of the Institute of Electrical and Electronics Engineers (IEEE). He has authored/co-authored over 90 technical papers and is an inventor on 5 patents.